Available online at www.sciencedirect.com
SCIENCE DIRECT®
Journal of Solid State Chemistry 173 (2003) 309–313
JOURNAL OF SOLID STATE CHEMISTRY
http://elsevier.com/locate/jssc

Structural distortions in the layered perovskites $CsANb_2O_7$ (A = Nd, Bi)

Alan Snedden,[a] Kevin S. Knight,[b,c] and Philip Lightfoot[a,*]

[a] School of Chemistry, University of St. Andrews, St. Andrews, Fife KY16 9ST, UK
[b] ISIS Facility, Rutherford Appleton Laboratory, Chilton, Oxon., OX11 0QX, UK
[c] Department of Mineralogy, The Natural History Museum, Cromwell Road, London SW7 5BD, UK

Received 17 October 2002; received in revised form 13 January 2003; accepted 18 January 2003

Abstract

Structural distortions in the layered perovskites $CsBiNb_2O_7$ and $CsNdNb_2O_7$, belonging to the Dion–Jacobson series, have been analyzed in detail using powder neutron diffraction. Both phases adopt the polar orthorhombic space group $P2_1am$, with neighboring perovskite-like blocks in 'eclipsed' conformation analogous to the tetragonal archetype $CsLaNb_2O_7$. The metric relationship between these distorted derivatives and the parent structure is $a_O \sim b_O \sim \sqrt{2}a_T$, $c_O \sim c_T$, with the orthorhombic distortion being due to off-center displacements of the A-site cation, together with cooperative BO_6 octahedral tilts. This mechanism of distortion is analogous to that in the Aurivillius phase ferroelectric $SrBi_2Ta_2O_9$, though the title compounds do not display ferroelectric behavior.

1. Introduction

Layered perovskite-related phases form the basis for many interesting classes of material, with a wide range of properties. The superconducting cuprates and giant magnetoresistive manganites are the most widely studied examples, both being based on the Ruddlesden–Popper structure type [1], which consists of a regular intergrowth of perovskite- and rocksalt-like building blocks, with general stoichiometry $[AO][ABO_3]_n$, or $[A_2][A_{n-1}B_nO_{3n+1}]$. Two closely related series of layered perovskites are the Aurivillius and Dion–Jacobson (DJ) series [2,3]. All three families have in common the $[A_{n-1}B_nO_{3n+1}]$ blocks of 'perovskite' structure, n octahedra thick. The difference lies in the intergrown blocks which separate the perovskite layers, viz. fluorite-like $[Bi_2O_2]$ units in the Aurivillius phases, and layers containing cations only (generally univalent) in the DJ series (i.e. $A'[A_{n-1}B_nO_{3n+1}]$). Typically, though not exclusively, the Aurivillius and DJ series incorporate d^0 cations (Ti^{4+}, Nb^{5+}, etc.) only at the B-site, and the consequent materials properties depend to a larger extent on the nature of the interlayer units; hence, the Aurivillius phases have been well-studied as ferroelectrics [4], whereas the DJ series have interlayer ion-exchange and ionic transport properties [5,6].

The detailed crystallographic nature of the Aurivillius phases has recently been well-established through a series of single-crystal X-ray [7,8] and powder neutron diffraction [9,10] studies. However, the crystallography of the DJ phases has been less well reported, and has been based on only a few good-quality single crystal [11] and PND [12] studies. Many papers have reported partial structural information based on powder X-ray diffraction measurements only. Consequently, there is some ambiguity and conflict in the exact nature of the crystallographic distortions present in these phases, with different superlattices being reported for similar compositions, in some cases. For example, Dion et al. [13] originally reported a $2 \times a$ superlattice for tetragonal $RbNdNb_2O_7$, whereas Kodenkandath et al. [14] more recently suggest the simpler $a \sim 3.87$ Å, $c \sim 10.9$ Å subcell, both studies being based only on powder X-ray diffraction data. Since such distortions often arise from subtle displacements of oxygen atoms (in particular 'octahedral tilt' type behavior) the preferred method of characterization is neutron rather than X-ray diffraction.

*Corresponding author. Fax: +44-1334-463-808.
E-mail address: pl@st-and.ac.uk (P. Lightfoot).

0022-4596/03/$ - see front matter © 2003 Elsevier Science (USA). All rights reserved.
doi:10.1016/S0022-4596(03)00096-3

Despite these problems, a simple generalization of the type of superlattice observed for a given A' cation has been given [15]. Three archetypal structures may be considered, depending on the relative alignment of neighboring perovskite layers: viz., eclipsed along the a- and b-axis (for $A' = Cs^+$, Rb^+) [11,12], eclipsed along a or b only ($A' = K^+$) [16] or staggered ($A' = Na^+$, Li^+, Ag^+) [17]. These differences arise from the coordination preferences of the A' cation, which varies from eight- to six- to four-coordinate for the three archetypes, respectively.

It is reasonable to suggest that the more subtle distortions within each of these families may be dictated by the nature of the A cation, specifically the size of A versus A' or B, and nature ('spherical' or non-spherical') of A, reminiscent of the range of distortions which occur in three-dimensional perovskites as a function of tolerance factor, etc. To explore this possibility we have carried out a detailed study, by PND, of the $n = 2$ DJ phases $CsBiNb_2O_7$ and $CsNdNb_2O_7$, which may be compared to the previously well-characterized analogues $CsLaNb_2O_7$ [11] and $RbLaNb_2O_7$ [12].

2. Experimental

Pure polycrystalline samples of $CsBiNb_2O_7$ and $CsNdNb_2O_7$ were prepared by solid-state reaction of stoichiometric quantities of $CsCO_3$ (20% molar excess), M_2O_3 and Nb_2O_5 which were thoroughly ground and heated at 1000°C for 24 h. Powder neutron diffraction data were collected at 25°C on the high-resolution diffractometer HRPD at the ISIS Facility, UK, with approximately 10 g samples packed in a thin-walled vanadium can. Data from both the 168° and 90° detector banks were used in the subsequent Rietveld analyses (GSAS [18]) leading to overall data ranges of $0.7 < d < 3.3$ Å.

3. Results and discussion

Previous work has provided a precise structural model for only one Cs-containing $n = 2$ RP phase, viz. the single-crystal X-ray study of $CsLaNb_2O_7$. This structure was refined in the archetypal $P4/mmm$ model, with $a_T \sim 3.9$ and $c_T \sim 11.2$ Å. From both our raw X-ray powder data and raw PND data it was immediately clear that this model was not appropriate for either of our materials, and a significant orthorhombic distortion was present. Indeed, Subramanian et al. [5] suggested a complex superlattice for $CsBiNb_2O_7$, involving cell doubling along each of the three crystallographic axes (i.e. $a = 7.599$, $b = 7.714$, $c = 22.738$ Å). On the other hand, Armstrong [12] suggested a different orthorhombic superlattice for $RbLaNb_2O_7$, involving a $\sqrt{2}a_T \times 2c_T \times \sqrt{2}a_T$ cell in space group $Imma$. Attempts to fit either of our PND data sets in these models were unsuccessful. Instead, it was found that a primitive cell corresponding to a simpler $\sqrt{2}a_T \times \sqrt{2}a_T \times c_T$ distortion was adequate to fit both phases, systematic absences being compatible with space groups $Pmam$ or $P2_1am$. Initial refinements in $Pmam$ converged to rather unsatisfactory fits ($\chi^2 = 24.9$ and 6.8 for $CsBiNb_2O_7$ and $CsNdNb_2O_7$, respectively) and led to some unusually large thermal parameters. Significant improvements in both fits, together with improvements in the behavior of the thermal parameters were found in the polar space group $P2_1am$, which was therefore adopted as the optimum model. In the final stages of refinement, oxygen atoms were treated anisotropically, metal atoms isotropically; for the Bi compound, a preferred orientation correction (along [001]) led to a significant improvement in the fit. A portion of the final Rietveld plot for $CsBiNb_2O_7$ is given in Fig. 1. The successful fit to superlattice reflections incompatible with either of the previous two structure types reported above is clearly highlighted. The full Rietveld plot for $CsNdNb_2O_7$ is given in Fig. 2. Structural details of these final models are presented in Tables 1–3 and Figs. 3–5.

The structural distortions are characterized by significant out-of-center shifts of both the A- and B-cations within the perovskitic site, with cooperative BO_6 octahedral tilting. Although the Nb cations display the 'ferroelectric'-type displacements typical of d^0 cations, leading to very short $Nb–O_{apical}$ bond lengths, the imposition of mirror symmetry perpendicular to the c-axis precludes any net polarization in this direction. However, the A-cation displacement does lead to a net polarization along the a-axis. This is analogous to the behavior in the Aurivillius phase ferroelectrics, such as

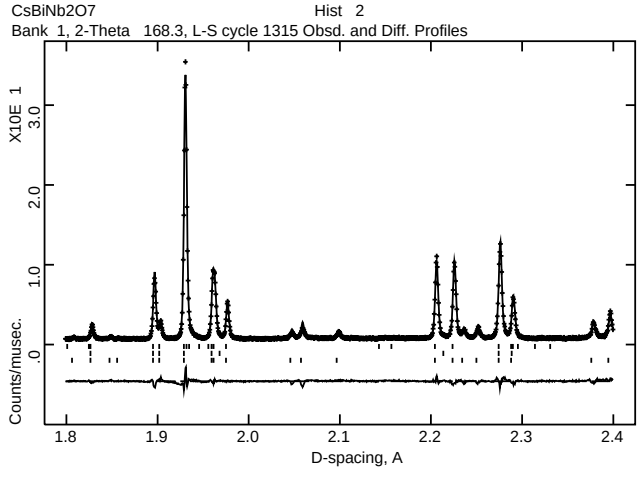

Fig. 1. Portion of the final Rietveld refinement for $CsBiNb_2O_7$. The lower set of tick marks corresponds to the refinement reported here, in $P2_1am$. The upper set and the middle set correspond to the variations previously reported for $RbLaNb_2O_7$ and $CsLaNb_2O_7$, for comparative purposes only.

$SrBi_2Ta_2O_9$ (space group $A2_1am$). However, a measurement of the dielectric behavior of $CsBiNb_2O_7$ by a.c. impedance spectroscopy demonstrates a rather low and temperature-independent dielectric constant ($\varepsilon_r \sim 4$), with no evidence for ferroelectric behavior.

Displacements within the *A*- and *B*-sites may be compared to those in the two-layer Aurivillius phases Bi_3TiNbO_9 [19] and $CaBi_2Nb_2O_9$ [20], both of which also show significant orthorhombic distortions (orthorhombicity values, $(2(a-b)/(a+b))$: 13.4, 4.5, 8.4 and 7.5×10^{-3}, for $CsBiNb_2O_7$, $CsNdNb_2O_7$, Bi_3TiNbO_9 and $CaBi_2Nb_2O_9$, respectively). The *B*-sites in the present DJ phases show significantly larger displacements towards the apical O-site than the Aurivillius phases (B–$O_{apical} = 1.82$ Å for both Bi_3TiNbO_9 and $CaBi_2Nb_2O_9$) demonstrating the need to compensate the relative 'underbonding' of the apical O site by the interlayer Cs cations; indeed the O(2) site actually becomes *overbonded* in the presents cases (Table 3). For the *A* cation sites the most extreme distortion is shown for $CsBiNb_2O_7$ (Fig. 5) and the smallest for $CsNdNb_2O_7$; the corresponding A–O equatorial distances are 2.33, 3.16 Å for $CaBi_2Nb_2O_9$ and 2.30, 3.18 Å for Bi_3TiNbO_9. These values directly follow the trends in orthorhombicity.

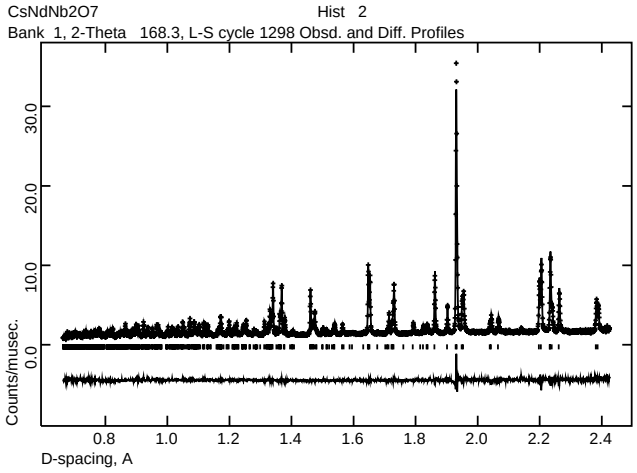

Fig. 2. Final Rietveld plot for $CsNdNb_2O_7$, 168° detector bank.

The octahedral tilt pattern involves in-phase rotation of adjacent octahedra around the *c*-axis, and out-of-phase rotation around the *a*/*b*-axes. This is analogous to the $a^-a^-c^+$ scheme (tilt system no. 10) in the Glazer notation for three-dimensional perovskites [21], and is also observed in the two-layer Aurivillius phases, e.g. $SrBi_2Ta_2O_9$ and $CaBi_2Nb_2O_9$. It is not surprising that $CsBiNb_2O_7$ displays octahedral tilting, and a very marked orthorhombic distortion, driven by the Bi^{3+} inert-pair effect. However, 'tolerance factor' arguments would perhaps suggest that related DJ phases such as $CsLaNb_2O_7$ and $RbNdNb_2O_7$ would also show a small

Table 1
Refined structural parameters for $CsBiNb_2O_7$ at 25°C, space group $P2_1am$, $a = 5.49528(7)$ Å, $b = 5.42251(7)$ Å, $c = 11.37663(14)$ Å. $R_{wp} = 0.063$, $\chi^2 = 7.6$, for 61 variables, $0.7 < d < 3.1$ Å

Atom	*x*	*y*	*z*	*U*(11)[a]	*U*(22)	*U*(33)	*U*(12)	*U*(13)	*U*(23)
Cs(1)	0.2536(7)	0.2590(5)	0.5	0.022(1)	0.022(1)	0.022(1)	0.0	0.0	0.0
Bi(1)	0.3046(3)	0.2776(4)	0.0	0.014(1)	0.014(1)	0.014(1)	0.0	0.0	0.0
Nb(1)	0.2456(4)	0.7577(4)	0.2078(1)	0.012(1)	0.012(1)	0.012(1)	0.0	0.0	0.0
O(1)	0.2157(5)	0.6840(5)	0.0	0.019(2)	0.013(2)	0.017(2)	−0.013(2)	0.0	0.0
O(2)	0.2474(4)	0.7797(4)	0.3617(2)	0.016(1)	0.011(1)	0.015(1)	0.011(2)	−0.011(2)	0.002(2)
O(3)	0.0099(5)	0.0267(4)	0.1604(2)	0.015(1)	0.028(2)	0.009(1)	0.009(2)	−0.006(2)	−0.006(2)
O(4)	0.4287(4)	0.4480(4)	0.1861(2)	0.035(2)	0.016(2)	0.028(2)	0.016(2)	−0.009(2)	−0.008(2)

[a] *Note*: all metal atoms refined isotropically.

Table 2
Refined structural parameters for $CsNdNb_2O_7$ at 25°C, space group $P2_1am$, $a = 5.47219(4)$ Å, $b = 5.44743(4)$ Å, $c = 11.16945(7)$ Å. $R_{wp} = 0.043$, $\chi^2 = 3.4$, for 60 variables, $0.7 < d < 3.3$ Å

Atom	*x*	*y*	*z*	*U*(11)[a]	*U*(22)	*U*(33)	*U*(12)	*U*(13)	*U*(23)
Cs(1)	0.2450(10)	0.2655(6)	0.5	0.020(1)	0.020(1)	0.020(1)	0.0	0.0	0.0
Nd(1)	0.2645(6)	0.2552(4)	0.0	0.009(1)	0.009(1)	0.009(1)	0.0	0.0	0.0
Nb(1)	0.2451(5)	0.7537(4)	0.2020(1)	0.010(1)	0.010(1)	0.010(1)	0.0	0.0	0.0
O(1)	0.2198(10)	0.6791(5)	0.0	0.024(3)	0.019(2)	0.028(2)	−0.004(2)	0.0	0.0
O(2)	0.2454(6)	0.8021(4)	0.3552(2)	0.016(1)	0.010(2)	0.018(1)	−0.005(2)	0.017(2)	−0.007(1)
O(3)	0.0072(6)	0.0278(6)	0.1443(2)	0.004(1)	0.024(1)	0.024(1)	0.001(1)	−0.009(2)	−0.005(2)
O(4)	0.4323(4)	0.4532(5)	0.1906(2)	0.027(2)	0.017(1)	0.022(1)	−0.010(2)	0.001(1)	−0.005(1)

[a] *Note*: all metal atoms refined isotropically.

Table 3
Bond distances (Å) and bond valence sums for $CsBiNb_2O_7$ and $CsNdNb_2O_7$

			$CsBiNb_2O_7$	$CsNdNb_2O_7$
Cs(1)	O(2)	×2	3.038(4)	2.988(4)
		×2	3.144(4)	3.198(6)
		×2	3.202(3)	3.202(6)
		×2	3.232(3)	3.341(4)
Nb(1)	O(1)		2.403(1)	2.297(1)
	O(2)		1.755(2)	1.731(2)
	O(3)		1.941(3)	1.972(5)
			2.024(4)	2.083(4)
	O(4)		1.973(3)	1.935(4)
			2.082(3)	2.053(4)
Bi(1)	O(1)		2.257(3)	2.322(4)
			2.269(3)	2.517(7)
			3.243(3)	3.002(7)
			3.256(3)	3.148(3)
	O(3)	×2	2.707(3)	2.473(4)
		×2	2.794(3)	2.596(3)
	O(4)	×2	2.409(2)	2.558(2)
		×2	3.311(3)	3.219(3)

BVS: Cs(1) 1.12, Bi(1) 2.97, Nb(1) 4.92, O(1) 1.89, O(2) 2.09, O(3) 2.00, O(4) 1.94.
BVS: Cs(1) 1.12, Nd(1) 2.99, Nb(1) 5.07, O(1) 1.74, O(2) 2.16, O(3) 2.11, O(4) 1.99.

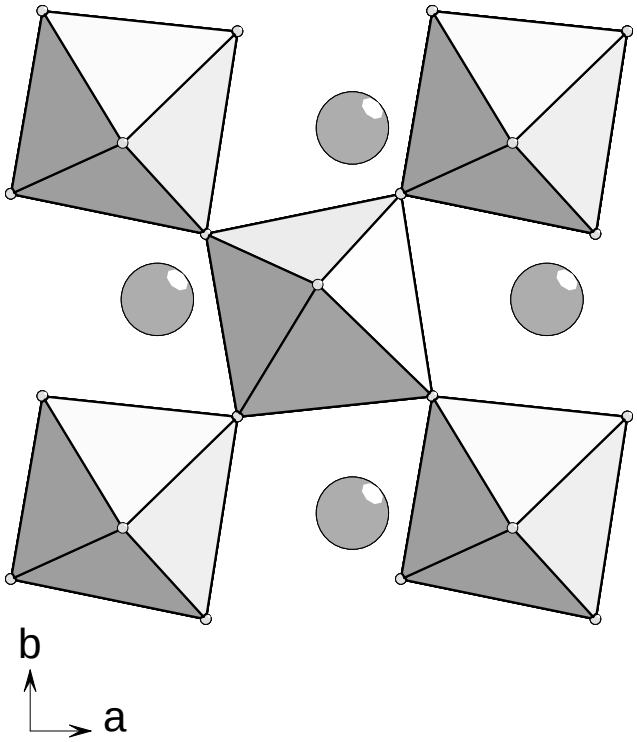

Fig. 4. Perovskite layer in $CsBiNb_2O_7$, viewed down the *c*-axis.

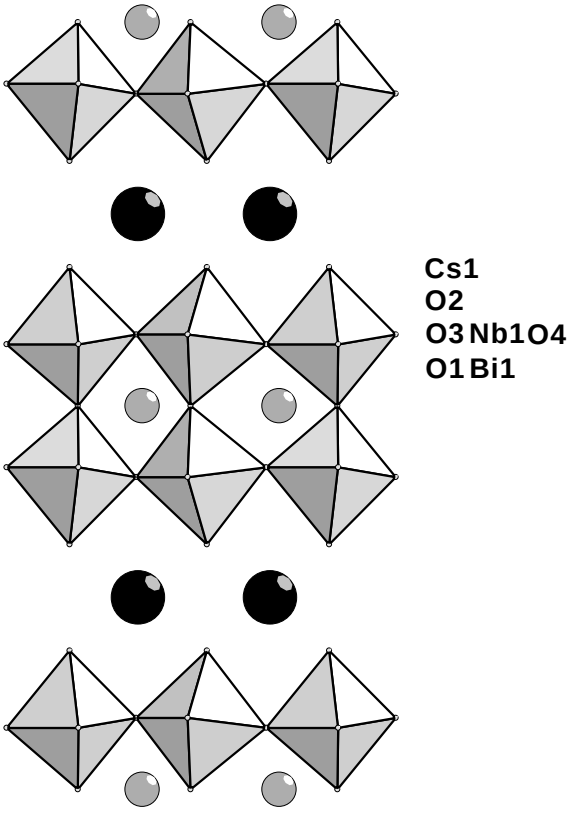

Fig. 3. Crystal structure of $CsBiNb_2O_7$.

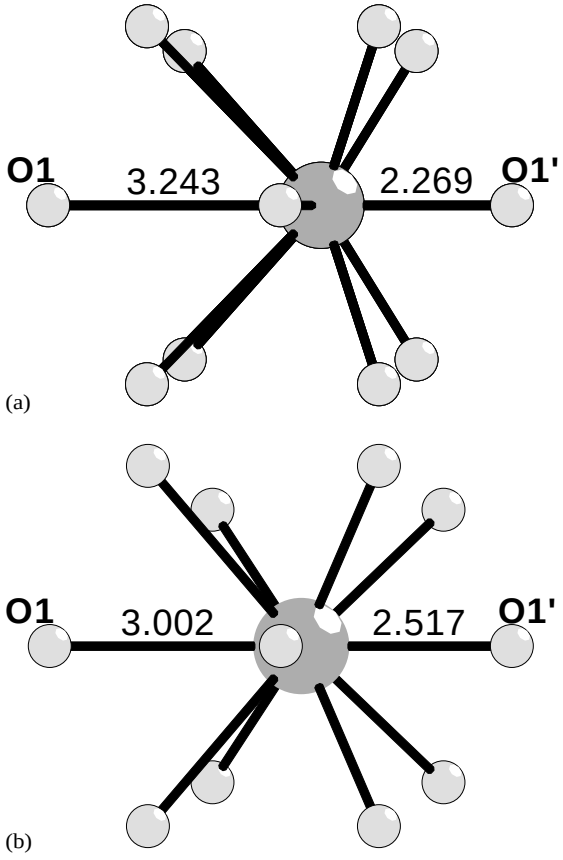

Fig 5. Local environment around the *A*-sites in $CsBiNb_2O_7$ and $CsNdNb_2O_7$.

distortion from the reported tetragonal symmetry. For example, the tolerance factor, t, for the [$SrNb_2O_7$] block in $SrBi_2Nb_2O_9$ is much larger (0.99) than that for the [$LaNb_2O_7$] block in $CsLaNb_2O_7$ (0.96). Despite this, the former shows a small orthorhombic distortion, whereas the latter does not. Bond–valence sum analysis [22] also suggests a small degree of underbonding, particularly at the La site in $CsLaNb_2O_7$ (BVS(La) = 2.88, BVS(Cs) = 0.98). These may be compared to the values in Table 3, where the distortions allow more optimal bonding at the *A*-site, at the expense of the Cs site. Further detailed structural work is clearly necessary to define more precisely the role of the *interlayer* units in these systems in influencing the behavior of the perovskite blocks.

In conclusion, we have shown that both $CsBiNb_2O_7$ and $CsNdNb_2O_7$ display a novel mechanism of distortion within the Dion–Jacobson family of layered perovskites. Large polar displacements of the perovskite *A* cation with cooperative octahedral tilting occur, reminiscent of the behavior in the Aurivillius phase ferroelectrics. The present compounds, however, appear not to exhibit ferroelectricity. In the light of the lack of definitive structural data on many related members of the DJ series, a more detailed study of the structural chemistry of these materials is merited.

References

[1] S. Ruddlesden, P. Popper, Acta Crystallogr. 10 (1957) 538.
[2] B. Aurivillius, Arkiv. Kemi. 1 (1949) 463.
[3] M. Dion, M. Ganne, M. Tournoux, Mater. Res. Bull. 16 (1981) 1429.
[4] C.A.P. de Araujo, J.D. Cuchiaro, L.D. McMillan, M. Scott, J.F. Scott, Nature (London) 374 (1995) 627.
[5] M.A. Subramanian, J. Gopalakrishnan, A.W. Sleight, Mater. Res. Bull. 23 (1988) 837.
[6] B.L. Cushing, J.B. Wiley, Mater. Res. Bull. 34 (1999) 271.
[7] R.L. Withers, J.G. Thompson, A.D. Rae, J. Solid State Chem. 94 (1991) 404.
[8] A.D. Rae, J.G. Thompson, R.L. Withers, A.C. Willis, Acta Crystallogr. Sect. B 46 (1990) 474.
[9] C.H. Hervoches, A. Snedden, R. Riggs, S.H. Kilcoyne, P. Manuel, P. Lightfoot, J. Solid State Chem. 164 (2002) 280.
[10] Y. Shimakawa, Y. Kubo, Y. Nakagawa, T. Kamiyama, H. Asano, F. Izumi, Appl. Phys. Lett. 74 (1999) 1904.
[11] N. Kumada, N. Kinomura, A.W. Sleight, Acta Crystallogr. Sect. C 52 (1996) 1063.
[12] A.R. Armstrong, P.A. Anderson, Inorg. Chem. 33 (1994) 4366.
[13] M. Dion, M. Ganne, M. Tournoux, Rev. Chim. Miner. 23 (1986) 61.
[14] T.A. Kodenkandath, A. Kumbhar, W.L. Zhou, J.B. Wiley, Inorg. Chem. 40 (2001) 710.
[15] J. Gopalakrishnan, V. Bhat, B. Raveau, Mater. Res. Bull. 22 (1987) 413.
[16] M. Sato, J. Abo, T. Jin, M. Ohta, Solid State Ionics 51 (1992) 85.
[17] K. Toda, M. Sato, J. Mater. Chem. 6 (1996) 1067.
[18] A.C. Larson, R.B. Von Dreele, Los Alamos National Laboratory, Report No. LA-UR-86-748, 1987.
[19] J.G. Thompson, A.D. Rae, R.L. Withers, D.C. Craig, Acta Crystallogr. Sect. B 47 (1991) 174.
[20] S.M. Blake, M.J. Falconer, M. McCreedy, P. Lightfoot, J. Mater. Chem. 7 (1997) 1609.
[21] A.M. Glazer, Acta Crystallogr. Sect. B 28 (1972) 3384.
[22] I.D. Brown, D. Altermatt, Acta Crystallogr. Sect. B 41 (1985) 244.